Enhancing 3D Indoor Visible Light Positioning With Machine Learning Combined Nyström Kernel Approximation

Vasileios P. Rekkas, *Graduate Student Member, IEEE*, Sotirios P. Sotiroudis, Lazaros Alexios Iliadis, *Graduate Student Member, IEEE*, Sander Bastiaens, Wout Joseph, *Senior Member, IEEE*, David Plets, *Member, IEEE*, Christos G. Christodoulou, *Life Fellow, IEEE*, George K. Karagiannidis, *Fellow, IEEE*, and Sotirios K. Goudos, *Senior Member, IEEE*

***Abstract*—Optical wireless communication (OWC) is emerging as a pivotal technology for next-generation broadcast networks, with visible light communication (VLC) poised to meet the escalating demands of advanced radio frequency systems. This study focuses on enhancing visible light positioning (VLP), recognized for its precision, simplicity, and cost-effectiveness, which are essential for accurate indoor localization and responsive location-based services. Central to our approach is the integration of advanced machine learning (ML) techniques, which fundamentally transform the accuracy and efficiency of 3D indoor positioning systems. We introduce an advanced VLP framework where ML is leveraged not merely as an adjunct but as the primary driver of innovation, significantly refining the processing of received signal strength (RSS) indicators. The methodology centers around a system comprising four light-emitting diodes (LEDs) arranged in a star geometry, optimized for precise spatial localization. We evaluate three distinct methodologies: a foundational star-shaped configuration for baseline position estimation, a repeated unit cell strategy to extend the four-LED configuration to a larger positioning area, and a sophisticated implementation employing Nyström kernel approximation. This integration of Nyström approximation into our ML framework drastically enhances the system's predictive accuracy, achieving an exceptional average relative root mean square error (aRRMSE) of 2.1 cm in a simulated setup. The results demonstrate that ML, especially combined with the application of the Nyström kernel approximation, significantly elevates the precision and operational efficiency of traditional VLP systems, setting new benchmarks for accuracy in indoor 3D positioning technologies and fostering advancements towards more sophisticated and adaptable communication networks.**

***Index Terms*—Visible light positioning (VLP), visible light communications, light-emitting-diode (LED) topology, machine learning (ML), Nyström kernel approximation.**

Manuscript received 1 March 2024; revised 21 July 2024; accepted 27 July 2024. This work was supported by the Hellenic Foundation for Research and Innovation (HFRI) under the 3rd Call for HFRI Ph.D. Fellowships under Grant 6646. *(Corresponding author: Sotirios K. Goudos.)*

Vasileios P. Rekkas, Sotirios P. Sotiroudis, and Lazaros Alexios Iliadis are with the ELEDIA@AUTH, School of Physics, Aristotle University of Thessaloniki, 541 24 Thessaloniki, Greece (e-mail: vrekkas@physics.auth.gr; ssoti@physics.auth.gr; liliadis@physics.auth.gr).

Sander Bastiaens, Wout Joseph, and David Plets are with the imec-WAVES Group, Department of Information Technology, Ghent University, 9052 Ghent, Belgium (e-mail: Sander.Bastiaens@ugent.be; wout.joseph@ugent.be; david.plets@ugent.be).

Christos G. Christodoulou is with the Department of Electrical and Computer Engineering, University of New Mexico, Albuquerque, NM 87131 USA (e-mail: christos@unm.edu).

George K. Karagiannidis is with the Department of Electrical and Computer Engineering, Aristotle University of Thessaloniki, 541 24 Thessaloniki, Greece, and also with the Cyber Security Systems and Applied AI Research Center, Lebanese American University, Beirut 03797751, Lebanon (e-mail: geokarag@auth.gr).

Sotirios K. Goudos is with the ELEDIA@AUTH, School of Physics, Aristotle University of Thessaloniki, 541 24 Thessaloniki, Greece, and also with the Department of Electronics and Communication Engineering, Bharath University, Chennai 600073, India (e-mail: sgoudo@physics.auth.gr).

Digital Object Identifier 10.1109/TBC.2024.3437216

I. Introduction

THE RAPID development of smart mobile devices, the Internet of Things (IoT), and artificial intelligence (AI) has made indoor location-aware services increasingly accessible. IoT-enabled devices and location-based services (LBS) have numerous applications in the commercial, industrial, and personal domains. These range from precise indoor navigation, virtual reality (VR), and augmented reality (AR) to streamlining production processes and guiding autonomous vehicles. The increasing demand underscores the crucial need for swift, dependable, and highly precise indoor wireless positioning. As outlined in releases 15 and 16 of the Third Generation Partnership Project (3GPP), forthcoming broadcasting networks must attain centimeter-level accuracy through emerging processes, technologies, and spectrum utilization [1].

In the field of outdoor positioning, the global positioning system (GPS) is established as the predominant technology. However, despite the accurate outdoor positioning of GPS, it is not suitable for indoor use cases, as GPS signals have weak received signal strength (RSS) and cannot penetrate the building's walls, as building materials impede the transmission of radio frequency waves [2], [3]. Additionally, GPS is unable to deliver equivalent levels of positioning accuracy, continuity, and reliability in indoor environments due to signal attenuation and reflection caused by buildings [4]. Therefore, more reliable systems are needed for indoor environments. Although various technologies have been proposed for indoor applications, such as wireless local area networks (WLANs), ultra-wideband (UWB), Zigbee, and Bluetooth, they are susceptible to electromagnetic signal interference generated by other radio frequency wireless devices and also require additional infrastructure.

Optical wireless communication (OWC) stands out as a compelling option for the final meter of wireless connectivity in broadcasting systems. It can function across an extensive spectrum, ranging from near-infrared to ultraviolet wavelengths, encompassing the visible light spectrum [5]. Visible light communications (VLC), as subdomain of OWC emerges as a promising technology in the coming 6G wireless networks [6]. Visible light positioning (VLP) is a VLC-based technology that has gained a lot of attention, as it can provide highly accurate estimation for indoor positioning systems (IPSs), compared with conventional technologies. VLP systems provide simultaneous communication and positioning services using light-emitting diodes (LEDs), which are power-efficient, cost-effective and have a long lifespan. Furthermore, VLP systems are immune to electromagnetic interference and can benefit from the free and unrestricted visible light portion of the spectrum, providing an accurate localization prediction.

The integration of VLC and VLP into broadcasting technology marks a substantial advancement in the realm of wireless communication systems. Utilizing the visible light spectrum, VLC offers enhanced data rates and secure communication channels, making it ideal for broadcasting applications where traditional radio frequency channels suffer from congestion and interference. This technology is applicable across various sectors, including intelligent transportation systems and industrial communications, where accurate device coordination and data broadcasting are paramount. By exploiting the visible light spectrum, VLP not only improves system efficiency but also enhances the reliability and scalability of broadcasting networks. Driven by advancements in light-emitting devices and optical receivers, this technology is poised to revolutionize broadcasting methodologies by delivering faster and more secure data transmission capabilities.

Recent studies have highlighted the potential of VLC and VLP in indoor broadcasting applications. Research indicates that VLC systems can effectively support wireless data access and indoor positioning, significantly enhancing the management and coordination of broadcasting equipment. Integrated systems leveraging VLC for data transmission and VLP for precise positioning offer robust communication solutions in dynamic environments [7], [8]. Furthermore, the development of Ethernet-VLC interfaces has expanded the applicability of VLC in professional broadcasting settings, thereby enhancing data communication capabilities [9].

In addition, adapting VLC technology for outdoor broadcasting through the use of streetlight infrastructure has broadened its scope to outdoor environments, enabling effective public safety communications and enhancing overall broadcasting capabilities [10]. Cooperative systems that combine VLC and VLP, employing advanced optical identification techniques, have demonstrated significant promise in improving both communication and positioning capabilities, making them highly effective for broadcasting in dynamic environments [11].

Several VLP-based signal features have been exploited to accurately estimate the indoor position, such as angle of arrival (AoA), time of arrival (ToA), time difference of arrival (TDoA), and RSS. AoA can provide highly accurate estimations but is rather complex as the receiver orientation and/or structure is essential. ToA and TDoA are computationally demanding, and to accurately predict position coordinates, they require strict synchronization between transmitters and receivers, while their distance in indoor scenarios is usually small [12].

RSS-based VLP systems have gained a lot of momentum as a promising candidate due to their simplicity, high centimeter accuracy, and low cost [13]. In an RSS-based VLP system, a photodiode (PD) is used to detect RSS values from various LEDs. The distance between the transmitter and the receiver can be obtained by analyzing the amplitudes or powers of the signals received from the LEDs. When the distance between transmitters and receivers increase, the measured power received decreases. Techniques such as trilateration can be applied for receiver coordinate estimation [14]. In RSS-based VLP systems, RSS measurements are given with unknown distances and heights based on channel modeling, making direct distance estimation particularly challenging for three-dimensional (3D) systems [15].

In non-ideal VLP scenarios, characterized by real-world complexities, factors such as interference, noise, fading, obstacles, and other variables disrupt the operating conditions. Shi et al. have shown that VLC system channel dynamics are significantly influenced by the non-linear and complex properties of gallium nitride (GaN) multiple quantum well (MQW) LEDs [16]. Their study details the substantial non-linear effects in illumination and data transmission, providing analytic formulations to evaluate LEDs' output illumination intensity and electro-optic signal responses at varying injection levels. These include carrier concentration derivations and considerations of leakage and recombination processes. Their model integrates an equivalent circuit approach, offering a comprehensive understanding of LED behavior. These insights reveal the limitations of conventional RSS-based channel modeling, often impractical for real-world applications due to their complexity. The developed model, validated with experimental data, emphasizes the critical interdependencies between the optical and electronic properties of LEDs, challenging simpler models that overlook such interactions. Extensive experimental validations within a VLC system align theoretical predictions with measurements, highlighting the sensitive dependence of VLC performance on specific LED properties and questioning the practicality of traditional approaches. Given that the calibration of RSS-based modeling is cumbersome in realistic environments, this suggests that utilizing machine learning ML on top of an RSS dataset might be an interesting and effective approach.

Given these insights, the combination of RSS data and machine learning (ML) has become an appealing alternative in the VLC community, offering accurate positioning estimates [17]. Unlike traditional methods that require detailed and often infeasible modeling of each LED's characteristics under varying operational conditions, ML algorithms can effectively handle complex and non-linear data. ML is a data-driven approach that provides accurate and robust results without the need to conscientiously quantify every parameter

of the VLP model or to exactly describe the underlying physical model [18]. This methodology not only simplifies the implementation but also enhances the adaptability and accuracy of localization in dynamic and challenging environments.

A. Motivation and Contributions

Classic LED configurations, such as the triangle [4], square or rectangle-shaped geometry cannot unambiguously solve the 3D VLP, while a star-shaped configuration is considered a better alternative for the 3D-position estimation [19]. The main contribution of this study is the innovative use of ML models to leverage RSS from carefully arranged LED setups for accurate 3D localization. This research centers on employing ML techniques to analyze and enhance the performance of existing LED configurations without modifying their physical structure, demonstrating notable enhancements in positioning precision.

In this work, a VLP system with four LEDs as transmitters forms a star geometry and a single PD as the receiver is used to predict the position coordinates of a mobile node. Three approaches are studied and compared to achieve an accurate 3D location of the receiver, using RSS values acquired in an experimental setup. The first approach uses the conventional star-shaped VLP system, which comprises four fixed LEDs to estimate the location of the PD, based on the acquired RSS values. In the second approach, a repeated unit cells methodology is utilized, by deploying different star configurations around the fixed LED with the highest mean RSS value. Thus, in this simulation, virtual transmitters are simulated in the entire room and corresponding RSS values can be obtained, offering more inputs to the ML models than the conventional four-LED configuration, increasing the positioning accuracy of the approach. In the final approach, Nyström kernel approximation is applied to the measured RSS values from the four transmitters (LEDs) to kernelize the ML regressors, mapping the described problem to a higher-dimensional kernel space. Thus, using the Nyström kernel approximation we model the problem using four inputs to obtain three outputs that are the 3D target coordinates. The main contributions of this work are listed below:

- Various ML models, namely RF, GBDT, Catboost, XGBoost, and LGBM, are utilized for comparing the performance of the 3D positioning system. Different conventional repeated unit cell methodologies are examined as an approach to formulate a wider vector of input (pseudo) RSS values.
- Implementation of the Nyström kernel approximation on the RSS values and comparison with a simple four-fixed LED star configuration. This approach performs well even when only a limited amount of training feature data is available, offering an improvement of up to 54% in terms of aRRMSE compared to the conventional four-LED configuration. Thus, Nyström kernel approximation is suitable for scenarios with a limited set of features, to provide accurate localization estimation.
- This work provides guidelines on the ill-posed problem of accurate 3D-position prediction with a limited number of input features in ML models. ML models, utilizing Nyström approximation can score accurate results close to the repeated cells methodology, but with significantly shorter computation time. Nyström realization can enhance the computation time, with respect to performance, up to 84% for the GBDT learner.

B. Organization of the Paper

The rest of this paper is structured as follows. Section II looks at related research, Section III outlines the system model, Section IV examines the methodology and approaches used, Section V covers machine learning techniques, Section VI presents the evaluation metrics and results, Section VII discusses the findings, and Section VIII summarizes the conclusions and potential future work.

Notation and abbreviations: In this study, lowercase Latin letters are utilized for scalars, matrices are denoted with bold capital letters, i.e., $\mathbf{U}$, and vectors with bold lowercase letters, i.e., $\mathbf{x}$. Table I presents the abbreviations in the study.

II. Related Work

Research into the use of ML techniques for wireless-based indoor positioning and RSS-based VLP systems has been extensive. This section lists the exploration work in the literature that applies and optimizes ML methods for VLP systems.

In [20], the authors contrast a traditional triangulation algorithm that relies on AoA with a data-driven Gaussian Process (GP) method for estimating 2D positions in visible light scenarios. In both methodologies, RSS data is gathered using a quadrant PD receiver equipped with an aperture, capturing image points from each transmitter on the PD. Subsequently, the location of the PD is predicted through the application of a least squares estimator and trigonometry. The GP-based approach achieves satisfactory positioning accuracy, with absolute errors of p_{50} and p_{95} of 3.62 and 16.65 cm for the 2D coordinates. In [18], a novel GP approach is proposed for RSS-based VLP systems. The proposed approach is compared with multi-layer perceptron (MLP) and multilateration (MLAT) methods on simulated data with random transmitter tilt and measured data. Both the MLP and GP approaches achieved higher positioning accuracy than the MLAT approach when there was a random tilt on the transmitter or a radiation pattern. GP achieves values of 0.82 cm and 3.12 cm for the 50th and 95th percentiles of error for a standard deviation $\sigma = 2^\circ$ in the simulations and 2.45 cm and 6.11 cm for the measured data. The limited amount of training data in the measured use case indicates that the proposed GP can be data-efficient for RSS-based VLP systems.

Liu et al. [21] introduce a hybrid algorithm incorporating extreme learning machine (ELM) and density-based spatial clustering of applications with noise (DBSCAN) for the estimation of a 2D position of a PD target, using a single LED. The PD is adjustable and measures angles relative to the LED projection point in conjunction with the RSS values. Initially, the random forest (RF) method is employed to categorize the area of interest into two segments: the corners zone and

TABLE I
ABBREVIATIONS

Abbreviation	*Definition*
2D	two-dimensional
3D	three-dimensional
3GPP	third Generation Partnership Project
AI	artificial intelligence
AoA	angle of arrival
AR	augmented reality
aRRMSE	average relative root mean squared error
CatBoost	categorical boosting
COB	chip on board
DBSCAN	density-based spatial clustering of applications with noise
ELM	extreme learning machine
EM	expectation-maximization
FDMA	frequency-division multiple access
GaN	gallium nitride
GBT	gradient boosted decision tree
GP	gaussian process
GPS	global positioning system
HPO	hyperparameter optimization
IoT	internet of things
IPSs	indoor positioning systems
kNN	k-nearest neighbors
LEDs	light-emitting diodes
LBS	location-based services
LGBM	light gradient boosting machine
MAE	mean absolute error
ML	machine learning
MLAT	multilateration
MLP	multi-layer perceptron
MRR	maximum received signal strength recognition
MQW	multiple quantum well
NNs	neural networks
OkNN	optimum kNN
OWC	optical wireless communication
PD	photodiode
RF	random forest
RFF	random fourier features
RMSE	root mean squared error
RRMSE	relative RMSE
RSS	signal strength
SVMs	support vector machines
TDoA	time difference of arrival
ToA	time of arrival
TPE	tree-structured Parzen Estimator
UWB	ultra wideband
VLC	visible light communication
VLP	visible light positioning
VR	virtual reality
WkNN	weighted kNN
WOkNN	weighted optimum kNN
XGBoost	extreme gradient boosting

the interior zone. In the interior zone, position inference is accomplished using the horizontal distance from the PD and angles. For the corner zone, the hybrid approach is applied. The ELM provides an initial estimate of the target's position, and as the rotatable PD is repositioned, the coordinates are re-estimated. Utilizing DBSCAN, the largest cluster, and its weight are determined, corresponding to the target's location, thereby reducing the positioning errors in the room from 11.97 to 1.94 cm. The proposed scheme demonstrates efficacy in compact spaces; however, its performance in larger rooms raises concerns due to potentially heightened processing latency, presenting significant challenges for real-time VLP systems. Moreover, the illumination intensity emitted by a single LED may prove inadequate for precise position estimation. In [22] an extreme learning machine (ELM) approach achieves an average 3D positioning error of 2.11 cm and 3.65 cm for simulation and real measured data case scenarios, while demanding ms-order average calculation times.

The authors in [23] propose a novel hybrid model by connecting k-nearest neighbors (kNN) and RF algorithms for VLP systems to determine the 2D coordinates of a PD receiver. The kNN method is employed to increase the RSS features, and the most significant ones are selected as inputs for the RF to mitigate complexity and computational expenses. The proposed approach attains an average positioning accuracy of 2 cm, surpassing other widely used kNN methods by fivefold. Notably, the authors achieve remarkable positioning precision, particularly away from the room center where prominent multipath reflections occur. This accomplishment considers various factors such as ambient light, thermal noise, and shot noise, along with the heightened reflection rate. In [24], the authors propose a hybrid approach for accurate 2D indoor positioning applications, based on RSS measurements. The proposed method consists of a maximum received signal strength recognition (MRR) technique and weighted optimum kNN (WOkNN) algorithm, by combining the optimum kNN (OkNN) and weighted kNN (WkNN). In this novel approach, the MRR is used to reduce computational time and the WkNN optimizes the positioning accuracy of the method. MRR led to a 42% to 52% reduction in computational time, depending on the number of k-neighbors, while WOkNN outperforms all conventional kNN-based approaches with a mean positioning error of 0.8 cm in the 2D VLP system.

Bakar et al. [2] propose a WkNN algorithm for two-dimensional (2D) localization estimation based on a dense RSS fingerprint dataset. The authors propose a custom board to drive four LED luminaries and obtain the RSS values at the receiver. During the experimental setup and data collection, at each location, the RSS at each PD for each of the four luminaries was measured, resulting in 16 RSS values. The positioning error could be reduced by using the Manhattan or Matusita distance metrics, leading to a median error of 4.74 mm for the 2D coordinates.

In [6], a second-order linear regressor and a kernel ridge regressor are proposed, utilizing a repeated unit cell methodology, where carrier frequencies f_1, f_2, f_3 are repeatedly deployed and reused to cover the entire positioning area of the laboratory. The linear regressor achieves a positioning error of 3.74 cm and 3.64 cm in the horizontal and vertical axes, while for the kernel ridge regressor, the errors are 2 and 2.23 cm respectively. To enhance the positioning accuracy of the proposed learners, a sigmoid function data preprocessing method is applied and studied. The introduction of the proposed preprocessing method reduces the positioning accuracy for the linear approach by 27.8% and 22% for horizontal and verτical axes, and for the ridge approach by 2% and 3.1% respectively. In [25], the authors propose a second-order regression ML and a polynomial trilateral ML learner to predict the 2D positioning in a VLP system using three LEDs. The VLP systems used a repeated cell approach to cover the positioning area, and the ML models are suitable for such relatively static environments. Both approaches provide a satisfactory positioning accuracy for use cases without optical background noise, with the positioning error within 4 cm when

TABLE II
PERFORMANCE COMPARISON OF VARIOUS 3D VLP SYSTEMS WITH COMPUTATIONAL COMPLEXITY AND REFERENCES

Reference	Accuracy (cm)	Computational Complexity	Methodology	Env.	Key Features
This Work	2.1	$O(k \cdot n \cdot d)$	XGBoost with Nyström kernel approximation	3D	Employs XGBoost with Nystrm approximation for efficient and precise 3D positioning
[20]	3.62-16.65	$O(n^3)$	Gaussian Processes with quadrant photodiode	2D	Improved accuracy with GP, using AoA and RSS
[21]	1.94-11.97	$O(n^2)$	Hybrid ELM and DBSCAN	2D	ELM initial estimates refined by DBSCAN for compact areas
[22]	2.11-3.65	$O(n^2)$	ELM	3D	Fast, accurate ELM in simulated and real data
[23]	2.00	$O(T \cdot v \cdot n \log(n))$	Hybrid kNN and RF	2D	kNN refines RSS for RF input, enhancing accuracy
[24]	0.8	$O(n \log n)$	Hybrid WOkNN with MRR	2D	MRR and WOkNN reduce time, improve accuracy
[2]	0.474	$O(n \log n)$	WkNN	2D	High accuracy from dense RSS fingerprints with WkNN
[6]	2.0-3.74	$O(n^3)$	Repeated unit cell with kernel ridge regression	3D	Repeated cell strategy with improved kernel regression
[25]	4-5	$O(n^2)$	Polynomial trilateral ML	2D	Effective in static environments without optical noise
[12]	1.92	$O(n \log n)$	wkNN with path-loss model	2D	Precise wkNN positioning via optimized path-loss model
[26]	3.8	$O(n \log n)$	Decision Trees	3D	Angles and RSS enhance 3D positioning accuracy with DTs

using the second-order regression ML and within 5 cm for the polynomial trilateral approach.

In [12], a wkNN approach is investigated to estimate the 2D location of a PD receiver using sparse fingerprints. The model is trained using an artificial dataset constructed based on a modified path-loss model. The path-loss exponent, which affects the attenuation of signals in wireless communication, is considered as a variable in this study. The optimal calibration of the path-loss exponent is achieved through bicubic interpolation, which helps fine-tune the model's performance.

Taking advantage of the wkNN approach with the fabricated RSS fingerprints, the study demonstrates an average positioning accuracy of 1.92 cm. This indicates the effectiveness of the wkNN method in accurately estimating the 2D location of the PD receiver in the given context. In [26], the authors explore and compare various ML methods for 3D indoor localization of a PD receiver. ML methods considered in the study include decision trees (DTs), support vector machines (SVMs), and neural networks (NNs). The localization is based on RSS fingerprints and the angles of a steerable laser source. All ML models in the study utilize RSS values, source angles, and the corresponding positions obtained from predetermined reference points to estimate the receiver's position. In particular, incorporating angles as input into the ML models leads to a reduction in the localization error. Among the ML methods evaluated, the DT model demonstrated the best performance, surpassing SVM and NNs. The DT model achieved an average positioning accuracy of 3.8 cm, indicating its effectiveness in accurately estimating the receiver's position in the indoor environment.

As illustrated in the performance comparison in Table II, the integration of the Nyström kernel approximation with the XGBoost algorithm significantly enhances computational efficiency without compromising accuracy. This melding of methodologies underpins an effective ML strategy crucial for innovations in 3D VLP systems.

The computational complexities are influenced by several key parameters:

- k denotes the number of trees in the XGBoost model, which significantly impacts the complexity and efficacy of the ensemble learning.
- n represents the number of samples in the dataset, a critical factor for algorithm scalability.
- d refers to the number of features in each sample, affecting the models' dimensionality and computational demands.
- T indicates the total number of trees in Random Forest models, essential for the robustness of ensemble methods.
- v represents the number of variables or features considered at each split in decision tree methods, crucial for precision in the decision-making process.

These variables are pivotal in defining the computational demands of each algorithm, showcasing how adaptability to data volume and feature complexity is crucial. A thorough understanding of these parameters is indispensable for fine-tuning the algorithms to ensure an optimal balance between accuracy and computational efficiency in 3D VLP applications. This advanced ML approach highlights a promising direction for both theoretical advancements and practical applications in the field.

III. SYSTEM FORMULATION

In the study, we consider the same configuration of a VLP system as in [13]. This configuration comprises four LEDs with a Lambertian radiation pattern with $m = 1$ set in a

starlike pattern within a room that measures 5×5 m and has a height of 3 m. Our assessment centers on the accuracy of 3D VLP by gauging the positioning error. This error is defined as the distance between the real position of the receiver and its calculated position using an untilted photodiode (PD)-based receiver with an active area of $A_R = 13\text{mm}^2$. This receiver is positioned on a uniform grid spaced 10 centimeters apart on the floor of the 5-meter by 5-meter space.

The white LEDs, identified as LEDi, ($i = 1..4$), are located at the coordinates $\mathbf{x_S} = (x_{S,i}, y_{S,i}, z_{S,i})$. These LEDs employ intensity modulation to emit separable beacon signals with distinct frequencies. Each LED sends out a signal that, upon reaching the point of interest, carries a received radiant power denoted $P_{R,i}$. A positioning method uses the received signal strength (RSS) values connected with the LED beacon emissions to estimate the position of the receiver, called $\hat{\mathbf{x}}$.

The VLP algorithm based on MLAT (Multilateration) functions in two main steps. First, it converts the set of $P_{R,i}$ values into a set of distances d_i between LED$_i$ and PD, achieved by inverting the VLP channel model previously introduced in [13]. Following this, the estimated position $\hat{\mathbf{x}}$ is determined by minimizing the least-squares error of the linearized system that links the distance set d_i to the LED coordinates $\mathbf{x_S}$, according to previous research.

In this sophisticated positioning system, the meticulous construction of the spatial environment and simultaneous collection of RSS measurements and positional data are critical initial steps. The refined distance estimates and RSS values, as processed through MLAT, serve as a sophisticated input for advanced ML models. These algorithms are meticulously engineered to dissect and comprehend intricate correlations within the RSS data. In executing this analysis, they refine the preliminary position estimates, substantially elevating the precision of the positioning system. This advancement illustrates the convergence of classical geometric positioning methods with modern ML techniques, thereby establishing a new benchmark for accuracy in indoor positioning systems. An interested reader could refer to [13] for further details.

IV. Methodology

In this work, three different methodologies are presented to predict The simulation environment for RSS measurement is constructed based on real-world data obtained from experiments conducted in the VLP lab at Ghent University, Belgium, as described in Section III and depicted in Fig. 1. These empirical measurements provided crucial parameters and configurations, ensuring that the simulations accurately mirror practical conditions. The data utilized for the ML models are simulated, generated from this realistic simulation environment, resulting in a comprehensive dataset consisting of 75,000 simulated position measurements to ensure robustness and accuracy in our analysis."

The four LEDs and the PD receiver are considered to be untilted and oriented horizontally and an overview of the visible light channel model is presented in Fig. 2. The PD is considered to be located in the xy-plane as presented in Fig. 2.

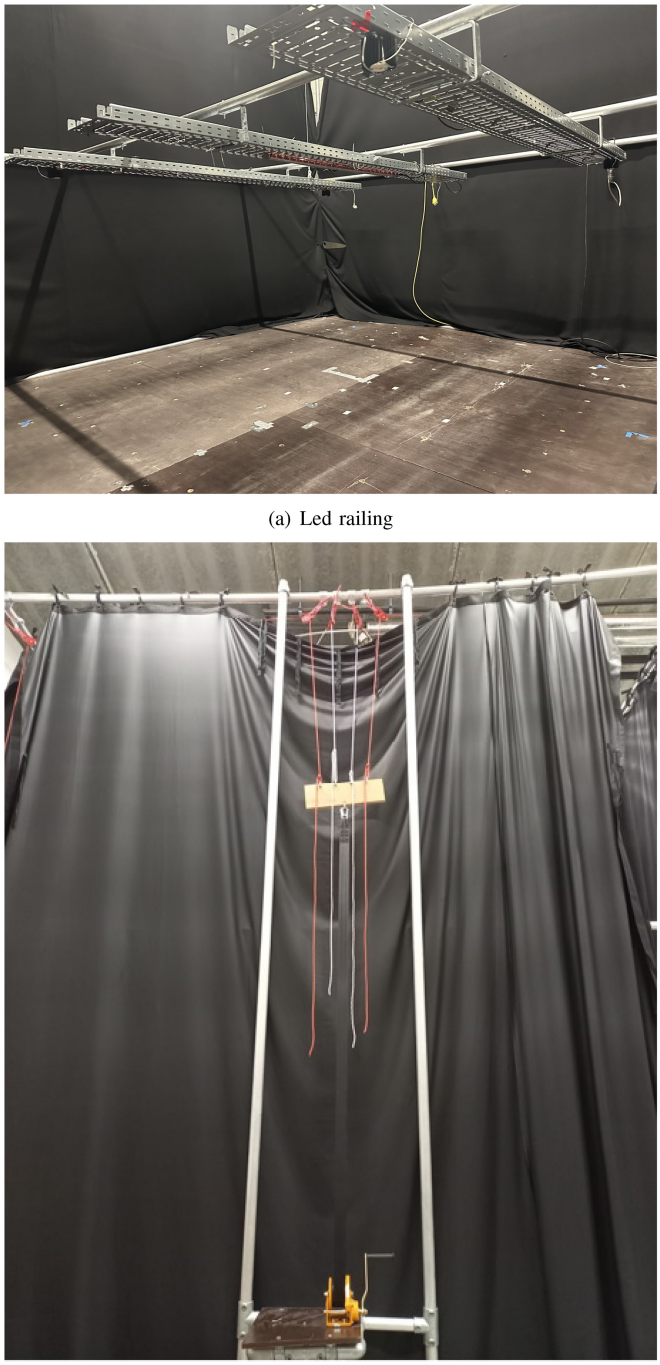

(a) Led railing

(b) Lab exterior view

Fig. 1. VLP lab.

This does not affect the generality of the approaches for the 3D positioning of the PD receiver.

In this study, several ML models are explored to analyze 3D position estimation within an indoor VLP system, considering various topology approaches. ML techniques are increasingly preferred over traditional methods due to their enhanced adaptability, superior capability in managing complex interactions, and robustness to noise and interference. Conventional methods often necessitate explicit environmental modeling and face challenges with non-linear interactions. In contrast, ML

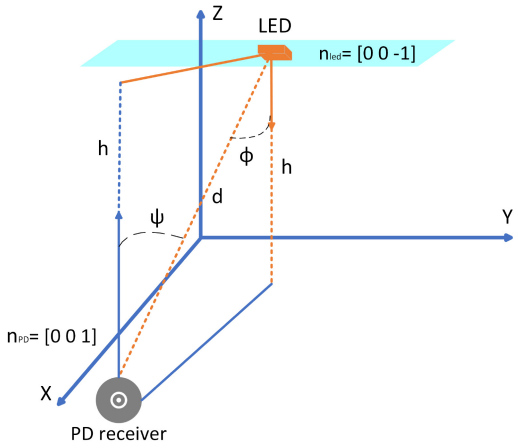

Fig. 2. Overview of the visible light channel model [13].

approaches can dynamically learn and adapt to environmental changes and intricate variable interactions, making them particularly suitable for the unpredictable conditions encountered in indoor VLP systems. Empirical evidence indicates that ML algorithms markedly enhance positioning accuracy and robustness in environments characterized by high noise levels, which are typical in indoor scenarios [17], [18].

The deployment of the ML models, such as random forest (RF), gradient boosted decision trees (GBDTs), extreme gradient boosting (XGBoost), light gradient boosting machine (LGBM), and categorical boosting (CatBoost), in VLP systems is strongly substantiated by their established efficacy in indoor positioning scenarios. RF is particularly esteemed for its robustness and precision in environments characterized by significant noise levels, making it highly effective for deciphering intricate data patterns [27]. GBDT algorithms, including XGBoost and LGBM, are adept at managing extensive datasets and modeling complex, non-linear relationships, thus ensuring high accuracy and computational efficiency [28]. CatBoost is distinguished for its proficiency in handling categorical data and its mechanisms to prevent overfitting, which can substantially enhance the precision of VLP systems [29]. The selection of these particular ML methods is based on their demonstrated effectiveness in addressing the distinctive challenges posed by VLP systems. These challenges include managing complex, non-linear interactions among multiple variables and achieving high-precision positioning in dynamic indoor environments.

A. Standard Star Configuration Approach

The first approach includes a standard 4-LED star VLP configuration, with the overview of the configuration depicted in Fig. 2. The four LEDs are considered to have known coordinates and be oriented horizontally while formulating a star-shaped configuration. The PD is considered to be located in the xy-plane and is considered to be untitled. The RSS measurements obtained from the PD receiver at all measurement points of interest are utilized for the ML models to estimate the 3D position of the receiver.

B. Repeated Cells Approach

In this approach, the standard star configuration of the four fixed LEDs is considered, and the whole positioning area will be covered by repeated unit cells for RSS augmentation. Based on the RSS measurement obtained from the PD receiver at all measurement points, the LED with the highest mean RSS values is fixed at a certain point x_i, y_i. Around this fixed LED four different star-shaped architectures are constructed, and at the same points of interest at the receiver, RSS measurements from all LEDs of all topologies are obtained. The set of four carrier frequencies (f_1, f_2, f_3, and f_4) employed within the star unit arrangement is used systematically throughout the positioning area, with the RF carrier frequencies being recycled and reused. Each LED possesses an individual identifier that is transformed through frequency up-conversion. Because distinct LEDs possess unique identifiers, it becomes possible to determine the position of each unit cell.

The repeated cells approach has been widely used in various problems for localization and positioning in VLC systems [2], [6], [18], [25], achieving satisfactory results in terms of average positioning error. The rationale of the repeated cells methodology is depicted in Fig. 3, where the fixed LED is presented as the black star, and each different star configuration is formulated around that LED. For the repeated cells approach, more cells are gradually added around the centered fixed LED, utilizing 4, 7, 10, and 13 LEDs that formulate 1, 2, 3, and 4 star-shaped topologies to obtain the RSS measurements.

C. Kernel Approximations

1) Kernel Methods: Kernel methods are highly effective learning techniques. They work by mapping data points into a feature space that can be high-dimensional or even infinite-dimensional. In this feature space, they find an optimal hyperplane with strong generalization capabilities. However, a drawback of kernel methods is their computationally intensive nature. The computational cost grows at least quadratically with the number of training examples due to the need to calculate the kernel matrix. Although approaches such as low-rank decomposition, or incomplete Cholesky decomposition, have been used to mitigate this computational challenge, the calculation of the kernel matrix remains necessary in these cases.

One popular strategy to avoid computing the kernel matrix is to simplify a kernel learning task into a linear prediction problem. This method revolves around forming a vectorized representation of the data, which provides an approximation of the kernel-based similarity between any two data points [30].

ML methodologies work better when the feature vector is large compared to the target vector [31]. In our problem's setup, four features (RSS values) exist for three outputs (3D coordinates). To overcome the challenges that arise from this framework, kernel approximation was utilized.

The kernel approximation refers to the transformation that finds a feature mapping to a higher-dimensional space [32]. Mathematically, one tries to find a feature mapping

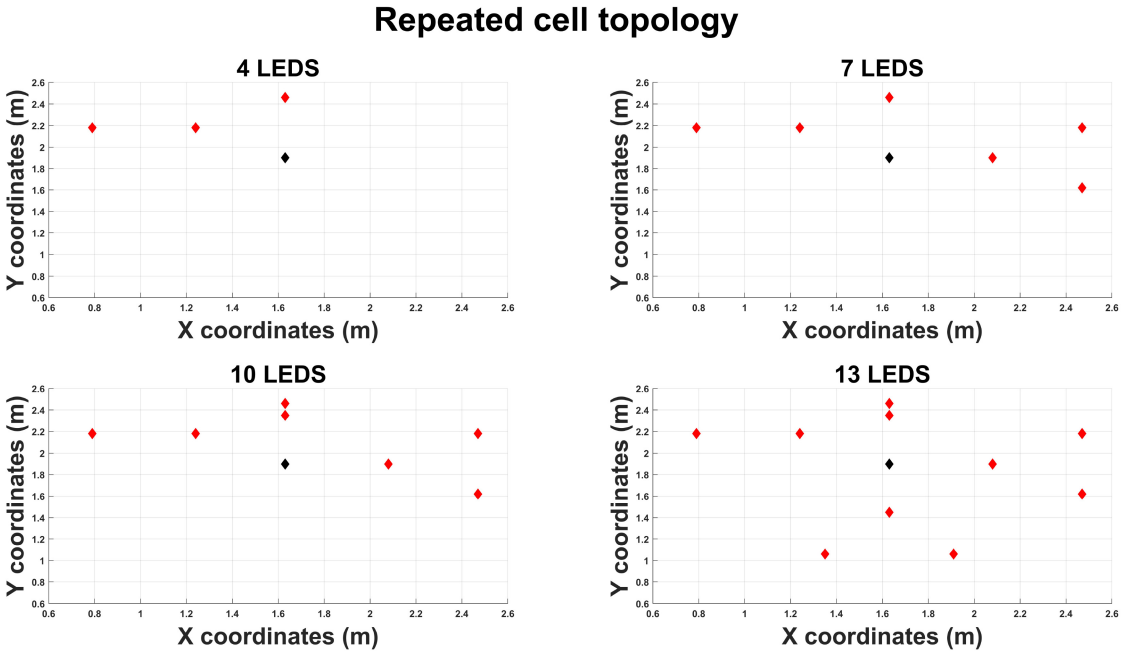

Fig. 3. Repeated cells topology.

$$\phi : \mathbb{R}^N \rightarrow \mathbb{R}^M, N < M$$

such that

$$k(\mathbf{v}, \mathbf{u}) \approx \phi(\mathbf{v})^T \cdot \phi(\mathbf{u}) \tag{1}$$

where $k(\mathbf{v}, \mathbf{u})$ is the kernel or the Gram matrix, which is the Hermitian matrix of inner products between vectors in an inner product space.

2) Nyström Kernel Eigenfunction Approximation Theory: The Nyström method is the most well-known technique for generating approximate vector representations. When these approaches are used, the computational burden associated with calculating the kernel matrix can be alleviated, making the learning process more efficient [30].

In the context of kernel machine theory, the covariance levels $k(\mathbf{v}, \mathbf{u})$ can be linked to an expansion in a feature space of dimension N, which surpasses the dimensionality of the input space $\mathbf{v}$. Here, u represents a vector variable in the feature space. This relationship is expressed as [33]:

$$k(\mathbf{v}, \mathbf{u}) = \sum_{i=1}^{N} \mu_i \psi_i(\mathbf{v}) \psi_i(\mathbf{u}) \tag{2}$$

where $N \leq \infty$, $\mu_i \geq 0$ represent the eigenvalues, and ψ_i represent the eigenfunctions of the operator, with a kernel $k(\mathbf{v}, \mathbf{u})$, so that:

$$\int k(\mathbf{v}, \mathbf{u}) \psi_i(\mathbf{v}) p(\mathbf{v}) d\mathbf{v} = \mu_i \psi_i(\mathbf{u}) \tag{3}$$

Here, $p(\mathbf{v})$ represents the probability of the input vector $\mathbf{v}$.

The eigenfunctions exhibit p-orthogonality, and can be described as follows:

$$\int \psi_i(\mathbf{v}) \psi_j(\mathbf{v}) p(\mathbf{v}) d\mathbf{v} = \delta_{ij} \tag{4}$$

where δ_{ij} is the Kronecker delta. To approximate the eigenfunction equation with an i-th sample $\{x_1, x_2, \ldots, x_w\}$, where w represents the number of samples or data points used in the approximation process, from $p(x)$, the integral over $p(x)$ is replaced by an empirical average, leading to:

$$\frac{1}{w} \sum_{k=1}^{w} k(\mathbf{u}, \mathbf{v_k}) \psi_i(\mathbf{v_k}) \approx \mu_i \psi_i(\mathbf{u}) \tag{5}$$

The p-orthogonality of the eigenfunctions results in the empirical constraint defined as:

$$\frac{1}{w} \sum_{k=1}^{w} \psi_i(\mathbf{v_k}) \psi_j(\mathbf{v_k}) \approx \delta_{ij} \tag{6}$$

and based on this equation, the matrix eigenproblem can be expressed as:

$$\mathbb{G}^w \mathbb{C}^w = \mathbb{C}^w \mathbb{D}^w \tag{7}$$

Here, $\mathbb{G}^w$ is the $w \times w$ Gram matrix with elements $K = K(\mathbf{v_i}, \mathbf{v_j})$ for $i, j = 1, \ldots, q$, $\mathbb{C}^w$ is the orthonormal column, and $\mathbb{D}^w$ is the diagonal matrix of entries ${\mu_1}^w \geq {\mu_2}^w \geq \cdots \geq {\mu_q}^w \geq 0$. Given the aforementioned equations 6, 7, the following approximations can be derived:

$$\begin{aligned} \psi_i(\mathbf{u}) &\approx \sqrt{w}\, \mathbb{C}^w_{j,i} \\ \mu_i &\approx \frac{{\mu_i}^w}{w} \end{aligned} \tag{8}$$

Equations 6, 8 can be utilized to derive the Nyström approximation, which characterizes the projection of a new point $\mathbf{v}$ into the i-th eigenvector within the feature space:

$$\psi_i(\mathbf{v}) \approx \frac{\sqrt{w}}{{\mu_i}^w} \sum_{k=1}^{w} k(\mathbf{v}, \mathbf{u_k}) \mathbb{C}^w = \frac{\sqrt{w}}{{\mu_i}^w} \mathbf{k_v} \phi_{\mathbf{i}}{}^w \tag{9}$$

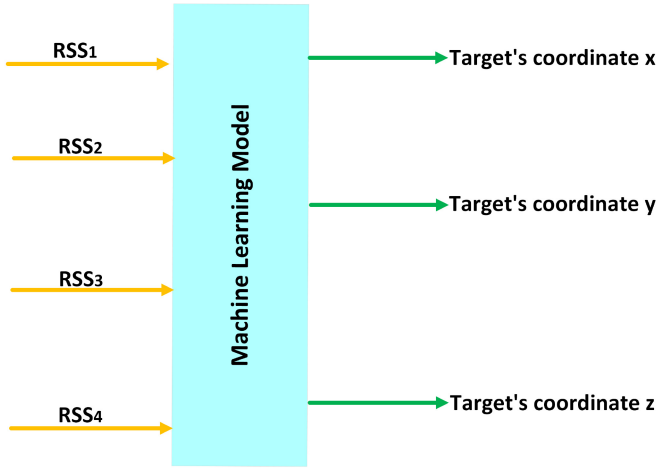

(a) 4-star configuration

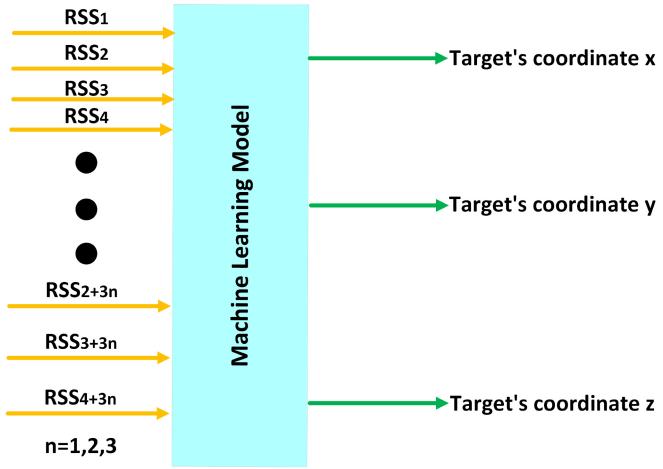

(b) Repeated cells configuration

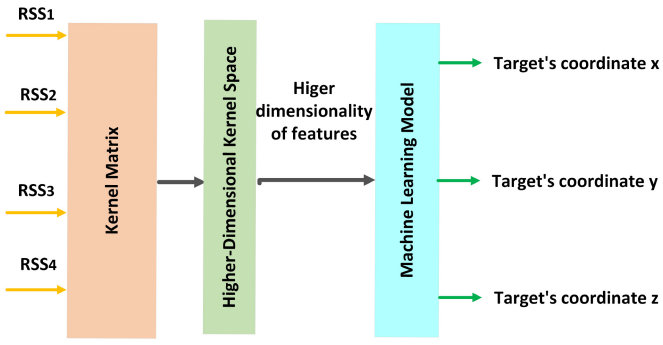

(c) Nyström kernel approximation

Fig. 4. Flow graphs: (a) 4-star configuration, (b) Repeated cells configuration, (c) Nyström kernel approximation.

where $k(\mathbf{v}, \mathbf{u_k})$ is the vector and $\phi_i{}^w$ the i-th column of $\mathbb{C}^w$ [33].

In our problem's setup, the RSS values from the four LEDs are treated as the input space $\mathbf{v}$. Nyström approximation transforms the input values to a higher dimensional space, based on the projection of the eigenvector in the feature space. The flow graphs of the proposed approaches are depicted in Fig. 4.

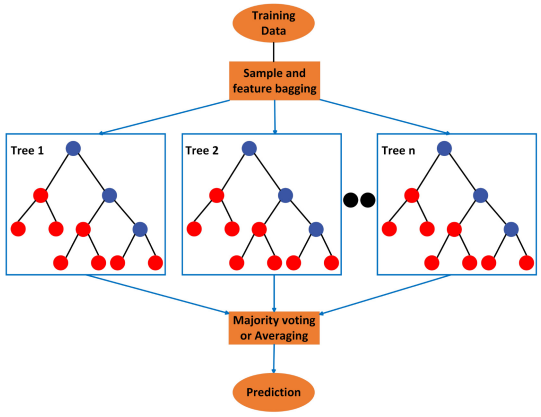

Fig. 5. Random Forest flowchart.

V. ML Techniques and Metrics

We have extensively explored several ML models in the context of wireless indoor positioning and the VLP configurations that we provide. In subsequent subsections, a detailed description of the sequential attributes of each ML method used in every approach is provided, which is based on RSS measurements for the VLP system. Utilizing the single four-LED topology, the repeated cell configuration, and the Nyström method, RSS values are obtained and used as inputs to every ML model.

A. Machine Learning Methods Description

1) Random Forest (RF): The Random Forest (RF) algorithm is an ensemble learning method that can be used for both classification and regression problems, such as VLP. Its operation entails creating numerous decision trees that utilize varying subsets of the dataset. The final prediction is determined by majority voting or averaging the results of these trees. Using this approach, RF improves the accuracy of the predictions and provides a means of controlling overfitting [34], [35]. The RF flow chart is depicted in Fig. 5

2) Gradient Boosted Decision Trees (GBDT): Gradient boosting decision trees (GBDT) is an ensemble method that combines several individual decision trees through a gradient boosting technique. It employs a boost method by aggregating predictions from multiple trees [28]. GBDT iteratively constructs new decision trees, following the gradient descent direction of the loss function from the prior decision tree model. It adjusts the errors introduced by the previously trained trees and trains new decision trees to capture the residual between the true value and the current prediction [28], [36]. GBDT has demonstrated satisfactory accuracy and efficiency in various applications and can be represented as a combination of multiple decision trees:

$$G(x) = G_0 + W_1 T_1(x) + W_2 T_2(x) + \ldots + W_M T_M(x) \quad (10)$$

where W_i represents the weight, G_0 is the initial value, and T_i represents the decision tree constructed in the i-th iteration.

3) Categorical Boosting (CatBoost): CatBoost is an advanced and high performance ML method that extends the GBDT approach. It utilizes binary symmetric or oblivious

Algorithm 1 CatBoost Pseudo-Code

Require: Model, $\{(\text{feature}_i, \text{target}_i)\}_n$, α, Loss, $\{\sigma_i\}_s$, Mode
Calculate gradients gradients using Loss and Model on target values
Select a random value r between 1 and s
if Mode is Plain **then**
  Initialize G as $\text{gradients}_r^{(i)}$ for $i = 1..n$
else if Mode is Ordered **then**
  Initialize G as $\text{gradients}_r^{(i)} - \sigma_{r-1}^{(i)}$ for $i = 1..n$
end if
Create an empty decision tree tree
for each step of top-down procedure **do**
  for each candidate split **do**
    Add the split to the tree structure
    if Mode is Plain **then**
      Compute $\Delta^{(i)}$ as the average of $\text{gradients}_r^{(p)}$ for instances p within the same leaf as instance i, for $i = 1..n$
    else if Mode is Ordered **then**
      Compute $\Delta^{(i)}$ as the average of $\text{gradients}_r^{(p)} - \sigma_{r-1}^{(p)}$ for instances p within the same leaf as instance i, for $i = 1..n$
    end if
  end for
end for

decision trees as weak learners to create a highly accurate model. The arrangement of feature points is randomized to produce various permutations, thus guaranteeing diversity among the combined input points, effectively preventing overfitting. An important enhancement in the CatBoost algorithm is its ability to automatically convert categorical features into numerical representations. Categorical features consist of distinct values or categories that are typically not directly comparable. In legacy preprocessing stages, categorical features are converted into numerical features by replacing them with numerical values [37]. The CatBoost approach process is analyzed in Algorithm 1.

4) Extreme Gradient Boosting (XGBoost): XGBoost is a scalable ML system that utilizes an ensemble approach with trees or linear classifiers. It combines multiple weak classifiers to create a more efficient and accurate model. XGBoost improves accuracy by optimizing the structured loss function through a second-order Taylor expansion. It also adjusts the weights of the training samples and utilizes the weights of the leaf nodes and the depth of the tree to effectively manage and reduce complexity. The popularity of XGBoost comes from its high accuracy, fast computation speed, and robustness in handling noisy data [38]. The objective function can be described as follows [37]:

$$\mathrm{F}(x) = \sum_{j=1}^{N} \left[\left(\sum_{j \in L_j} g_j \right) o_j + \frac{1}{2} \left(\sum_{j \in I_j} h_j + \alpha \right) o_j^2 \right] + \beta N \quad (11)$$

where I_j the leaf samples in node i, L_j denotes the set of samples belonging to the j-th leaf node, β is the complexity parameter, N the number of tree leaves, α the penalty parameter, o_j the leaf nodes output, and g_j, h_j the first and second derivatives of the loss function.

5) Light Gradient Boosting (LGBM): LGBM is a histogram-based ensemble decision tree algorithm that improves model efficiency, decreases execution time, and conserves memory resources on a machine. It uses a leaf-wise splitting approach to build the tree vertically, alongside a histogram-based technique to identify optimal split parameters and minimize standard deviations [39]. Unlike conventional tree growth, LGBM chooses the leaf with the greatest growth loss, allowing for a more efficient and effective tree construction process. This approach results in the development of a final tree model that achieves superior performance. The objective function minimization process in LGBM utilizes the second-order approximation, allowing for rapid optimization of the objective function. This approximation method facilitates efficient and effective optimization, resulting in rapid convergence toward the optimal solution [39].

The LGBM method was developed based on XGBoost using N additive functions to forecast the output. In the context of a provided input dataset featuring N data instances, the anticipated output of the i-th instance is represented as:

$$\bar{y}_i = \phi(x_i) = \sum_{j=1}^{N} f_j(x_i), \quad f_j \in G \quad (12)$$

x_i is the data instance, G denotes the function space encompassing the regression trees, and each f_k represents an individual and separate regression tree. The algorithm aims to minimize the objective function, which can be described as:

$$O = \sum_i L(\bar{y}_i, y_i) + \sum_j \Psi(f_k) \quad (13)$$

L is the loss function, y_i is the target value; and $\Psi(f_k)$ the regularization term.

B. Metrics

To evaluate the performance of the ML algorithms used for position estimation, various error metrics can be used. These metrics quantify the disparity between the predicted positioning values and the corresponding values in the test set data. Since the models in question employ multiple output regression techniques, suitable performance metrics encompass the relative root mean square error (RRMSE) and the average relative root mean square error (aRRMSE). These metrics are defined as follows:

$$RRMSE_i = \sqrt{\left(\frac{\sum_{k=1}^{q} \left(z_k - \hat{z}_k\right)^2}{\sum_{k=1}^{q} \left(z_k - \bar{z}_k\right)^2} \right)} \quad (14)$$

$$aRRMSE = \frac{1}{s} \sum_{i=1}^{s} RRMSE_i \quad (15)$$

where q represents the number of input records in the test set, z_k represents the actual measured data, $\hat{z}$ represents the predicted values for the k-th data record, $\bar{z}_k$ represents the average of the actual values for the target variable and s

represents the number of output variables and $RRMSE_i$ is the RRMSE at each of the output variables (in our case $i = 3$ for the axes x, y, z). These metrics provide additional information when dealing with multiple-output regression models.

C. Optuna

Optuna is an advanced hyperparameter optimization (HPO) framework that features a define-by-run API. It offers dynamic parameter search space construction through efficient search and pruning strategies [40]. In this study, the Tree-structured Parzen Estimator (TPE) algorithm is used, a single-objective Bayesian optimization method. TPE is utilized to explore and find optimal combinations of hyperparameters to minimize the RRMSE. TPE employs a tree-structured approach to model the hyperparameter distribution and efficiently explore the search space based on observed trial results. The algorithm achieves this by repeatedly evaluating the objective function with different parameter values [41].

The optimization process can be described as follows [40]:

- Identify the optimization direction, parameter type, permissible range, and maximum count of iterations.
- Choose a population of individuals evenly distributed throughout the specified range of parameter values.
- Terminate unpromising individuals based on predefined trimming conditions using a trimmer.
- Evaluate the objective function for the remaining individuals in the population.
- Iterate through the previously outlined steps until the designated maximum iteration count is achieved.
- Output the best solution and the corresponding value of the function.

Optuna is gaining recognition due to its ability to provide an optimal combination of hyperparameters at a relatively lower computational cost compared to other optimization methods such as random grid search and grid search cv [40].

VI. Experiments and Results

The primary objective of this study is to accurately predict the 3D position of the PD receiver. To achieve this, various ML algorithms were compared, namely GBDT, Catboost, XGBoost, RF and LGBM, and the best-performing model, namely XGBoost, was selected. A dataset of 75, 000 position measurements was prepared, each measurement consisting of the receiver's x, y, and z coordinates and RSS values from the LEDs arranged in a star formulation, in a room with dimensions 5 m $\times$ 5 m $\times$ 3 m. The RSS measurements of the approaches are obtained in a simulation environment constructed based on experiments conducted within a VLP lab at Ghent University, Belgium. As in [13], the LED plane is equipped with four BXRE-35E2000-C-731 chip-on-board (COB) LEDs, controlled by LTM8005 Demo Boards to implement the square wave-based frequency-division multiple access (FDMA) scheme. The modulation frequencies, denoted as $f_{c,i} = 2^{(i-1)} \times f_0$ (where i ranges from 1 to 4), are dictated through Wi-Fi using the Adafruit Feather M0 WIFI w/ATWINC1500. Here, f_0 is set to 1 kHz to avoid inducing flicker. The receiver plane is equipped with a Thorlabs PDA36A24 PD receiver, with a trans-impedance gain set to $1.51 \times 10^5 V/A$). Data are preprocessed utilizing a scaler to enhance the performance of the ML models. The complete preprocessed dataset of 3D positions and RSS values was randomly split into two separate datasets: the training dataset, which comprised 80% of the total data, and the testing data set, which represented the remaining 20%. The test set was used to evaluate and validate the performance of each learner.

A. Data-Preprocessing

To preprocess the data and improve positioning accuracy, a min-max scaler was applied to the pipeline of the ML models under test. Min-Max normalization is a linear transformation applied to the original data. In this process, minimal and maximal boundaries are set for the values, and the entire dataset is rescaled to fit within the range. The threshold value for Min-Max normalization typically ranges from zero to one. Scaled data A_{scaled} can be expressed as:

$$A_{scaled} = \frac{A - min(A)}{max(A) - min(A)} \tag{16}$$

One benefit of using the Min-Max scaler is that it enables us to standardize features within the same range, even if they initially have vastly different values. This ensures that all information is retained, as the relative distance ratios between the data points are preserved. For algorithms that depend on measuring the distance between points, this scaling method allows the inclusion of features with small and large values without losing their significance [42].

B. Numerical Results

A quantitative evaluation of five well-established ML predictors, namely RF, GBDT, CatBoost, XGBoost, and LGBM, is conducted. To optimize the hyperparameters of each ML model, the Optuna framework is utilized. Three different methodologies are presented for a star-shaped configuration consisting of four fixed LEDs, aiming to obtain accurate indoor VLP estimation:

- A simple star-shaped configuration consisting of four fixed LEDs.
- The conventional repeated unit cells methodology, to formulate a wider vector of input (pseudo) RSS values, with three approaches being conducted. The number of LEDs (thus the input RSS values) gradually increases, with seven, ten, and thirteen RSS values being explored as input to the ML models.
- The Nyström kernel approximation method with a chi-squared kernel being utilized to transform the input four RSS values of the standard star configuration, into a higher-dimensional space, to estimate the 3D position of the PD receiver. The proposed Nyström approximation constructs the higher-dimensional space map with a number of 40 features as transformed representations of the original RSS values and these can be used as input

TABLE III
4 LEDS APPROACH

Algorithm	Single 4 LEDs topology	
	aRRMSE (cm)	Time (s)
GBDT	7.5	42
CatBoost	5.1	179
XGBoost	3.8	131
RF	8.9	60
LGBM	4.3	15

TABLE IV
NYSTRM KERNEL APPROXIMATION METHOD APPROACH

Algorithm	Nyström approximation	
	aRRMSE (cm)	Time (s)
GBDT	5.6	75
CatBoost	2.4	237
XGBoost	2.1	48
RF	5.5	122
LGBM	2.7	17

features for the models, while the kernel is a commonly used chi-squared function, that can be expressed as:

$$K(X, Y) = \exp\left(-\gamma \sum_{i=1}^{n} \frac{(x_i - y_i)^2}{x_i + y_i}\right) \quad (17)$$

where $K(X, Y)$ is the chi-squared kernel value between vectors X,Y, γ is a positive constant that controls the kernel's shape, n is the number of elements in the vectors X and Y, while x_i and y_i are the corresponding elements in the vector.

The ML models are examined and evaluated for the different approaches in the VLP system under study, based on various error metrics. The training procedure utilizes the performance and capabilities of an NVIDIA RTX 3080 GPU.

The models for the first methodology are fine-tuned using the Optuna framework, based on the four RSS input values, and the hyperparameters remain the same for the Nyström approximation in order to highlight the great accuracy performance it provides. For the repeated cells methodology, as the input RSS values are increased, the hyper-parameters are selected based on the Optuna framework in every case.

The results are shown in Tables III,IV,V for a single topology, repeated cells, and Nyström kernel approximation method for the different ML models, based on the aRRMSE and the computation time for the training of each model. Fig. 6 represents the error and comparison for the best learner, namely XGboost, for each of the methods utilized to train the ML models.

VII. DISCUSSION

Significant research efforts have focused on overcoming the challenges of localization and positioning in VLC systems, through the application of AI and especially ML methods. In this study, three distinct approaches are introduced for a star-shaped arrangement consisting of four fixed LEDs, to achieve precise estimation in an indoor VLP system.

When utilizing the conventional repeated unit cells methodology, the ML methods outperform, as expected, the simple

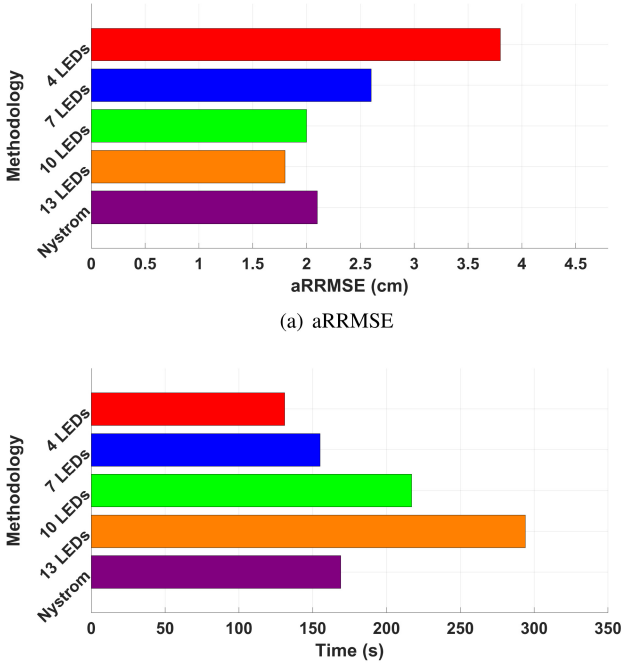

(a) aRRMSE

(b) Time

Fig. 6. XGBoost comparison performance: (a) aRRMSE, (b) Time.

star-shaped configuration consisting of four fixed LEDs. The accuracy is enhanced as the number of LEDs (inputs to the ML models) increases, up to 53%, at the cost of computation time, as there is an increase of up to 10 times.

The Nyström kernel approximation method can achieve better results than repeated cell methodologies with seven and ten LEDs, and similar results with the more complex 13 input LED methodology, with a shorter computation time, as observed in Tables III and IV. This methodology can address the ill-posed task of precise 3D-position prediction using a restricted set of input features within the ML models, without the need to use more than four input RSS values, thus reducing the computation time and complexity. To see if the suggested Nyström kernel approximation method works in other situations, Fig. 7 shows how well the method works for XGBoost (in terms of aRRMSE) as the training data set grows. The aRRMSe of the Nyström method is significantly reduced compared to the conventional four-LED approach, for small training samples. We notice that the Nyström method achieves at least $2cm$ lower aRRMSE for all possible training sizes, showcasing its superior performance, even for smaller training datasets.

The temporal metrics pertinent to our experimental results primarily reflect offline processing periods necessary for the training of ML algorithms and initial data preprocessing. These foundational stages are crucial for the precise calibration and systematic configuration of the system prior to its deployment. In contrast, online processing periods, which are essential for applications requiring immediate system responses such as navigational systems or real-time monitoring, are characterized by the latency from data capture to positional computation in operational environments. While the scope of this study did

TABLE V
REPEATED CELLS APPROACH

Algorithm	7 input LEDS		10 input LEDS		13 input LEDS	
	aRRMSE (cm)	Time (s)	aRRMSE (cm)	Time (s)	aRRMSE (cm)	Time (s)
GBDT	6.6	313	5.2	327	4.7	478
CatBoost	4.3	214	3.6	284	3.1	716
XGBoost	2.6	155	2.18	217	1.88	294
RF	7.9	79	6.3	106	4.8	198
LGBM	4.0	17	3.5	18	3.0	20

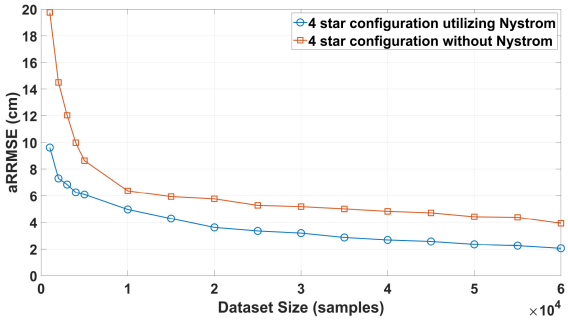

Fig. 7. XGBoost comparative performance vs training dataset size with (blue line) and without (red line) Nyström approximation.

not encompass these online processing metrics, they remain critical for assessing the practical effectiveness and real-world applicability of the system in dynamic environments.

Both the conventional repeated cell methodology and the Nyström methodology for all ML models provide aRRMSE values below 10 *cm*, which is a satisfactory result for a multi-output problem [43].

The findings of our work suggest that Nyström kernel approximation method combined with ML approaches can offer highly accurate 3D localization prediction in an indoor VLP system with much lower computation time and complexity than conventional methods. Repeated cells methodology can also provide accurate results when utilizing ML methods in exchange for a longer processing period. All approaches, however, can offer highly accurate 3D position estimations with respect to computation complexity and time.

However, our work has certain limitations. First, a lot of data pre-processing is required to create the database of the RSS values for each scenario. Furthermore, deep learning (DL) models are not included in this comparative study, but complicated DL and ML models could offer increased accuracy in 3D position estimation. Additionally, each ML model needs to be fine-tuned for different RSS inputs and topologies, increasing the computation cost and time for this comparative study. Finally, the reported processing times pertain solely to offline model training and data preprocessing, excluding online processing crucial for real-time applications. Subsequent studies are required to explore these metrics to rigorously evaluate the system's real-world performance.

VIII. CONCLUSION

In this work, various ML models are studied for the 3D position estimation in an indoor VLP system for different topology structures. Conventional repeated cells and Nyström kernel approximation methods are used and compared to achieve positioning accuracy below 8 *cm* for all ML models, and smaller than 2 *cm* for the most accurate learner, namely XGBoost. Both approaches can offer highly accurate 3D location predictions, with respect to computation time.

Nyström kernel approximation achieves similar estimation results compared to the more complex repeated cells methodology with more LED inputs. Thus, our approach provides a solution to the challenging task of precise 3D position prediction using a restricted set of input characteristics for the ML models. The future work of this study includes utilizing more complex ML and deep learning (DL) models. Furthermore, we plan to apply other kernel approximations such as Nyström expectation-maximization (EM) or Random Fourier Features (RFF), and analyzing larger indoor spaces for position estimation. Additionally, as part of future work, exploration of input approximation and ML models can be carried out for the estimation of both the 3D position and the tilt angles of the PD receiver.

REFERENCES

[1] B. Meunier et al., "Visible light positioning with lens compensation for non-Lambertian emission," *IEEE Trans. Broadcast.*, vol. 69, no. 1, pp. 289–302, Mar. 2023.
[2] A. H. A. Bakar, T. Glass, H. Y. Tee, F. Alam, and M. Legg, "Accurate visible light positioning using multiple-photodiode receiver and machine learning," *IEEE Trans. Instrum. Meas.*, vol. 70, pp. 1–12, 2021.
[3] K. Ali et al., "Measurement campaign on 5G indoor millimeter wave and visible light communications multi component carrier system," *IEEE Trans. Broadcast.*, vol. 68, no. 1, pp. 156–170, Mar. 2022.
[4] L. Shi et al., "5G Internet of Radio light positioning system for indoor broadcasting service," *IEEE Trans. Broadcast.*, vol. 66, no. 2, pp. 534–544, Jun. 2020.
[5] L. Shi, B. Béchadergue, L. Chassagne, and H. Guan, "Joint visible light sensing and communication using m-CAP modulation," *IEEE Trans. Broadcast.*, vol. 69, no. 1, pp. 276–288, Mar. 2023.
[6] Y.-C. Wu et al., "Received-signal-strength (RSS) based 3D visible-light-positioning (VLP) system using kernel ridge regression machine learning algorithm with sigmoid function data preprocessing method," *IEEE Access*, vol. 8, pp. 214269–214281, 2020.
[7] H. Yang, "Visible light communication systems supporting wireless data access and indoor positioning applications," Ph.D. dissertation, School of Electrical and Electronic Engineering, Nanyang Technol. Univ., Singapore, 2020.
[8] L. -S. Hsu et al., "Using received-signal-strength (RSS) pre-processing and convolutional neural network (CNN) to enhance position accuracy in visible light positioning (VLP)," in *Proc. Opt. Fiber Commun. Conf. Exhib. (OFC)*, 2022, pp. 1–3.
[9] F. Delgado, I. Quintana, J. Rufo, J. A. Rabadan, C. Quintana, and R. Perez-Jimenez, "Design and implementation of an Ethernet-VLC interface for broadcast transmissions," *IEEE Commun. Lett.*, vol. 14, no. 12, pp. 1089–1091, Dec. 2010, doi: 10.1109/LCOMM.2010.12.100984.
[10] H. B. Eldeeb and M. Uysal, "Visible light communication-based outdoor broadcasting," in *Proc. 17th Int. Symp. Wireless Commun. Syst. (ISWCS)*, 2021, pp. 1–2, doi: 10.1109/ISWCS49558.2021.9562235.

[11] J. Chen and X. You, "Visible light positioning and communication cooperative systems," in *Proc. 16th Int. Conf. Opt. Commun. Netw. (ICOCN)*, 2017, pp. 1–3, doi: 10.1109/ICOCN.2017.8121463.

[12] I. M. Abou-Shehada, A. F. AlMuallim, A. K. Al Faqeh, A. H. Muqaibel, K.-H. Park, and M.-S. Alouini, "Accurate indoor visible light positioning using a modified pathloss model with sparse fingerprints," *J. Lightw. Technol.*, vol. 39, no. 20, pp. 6487–6497, Oct. 15, 2021.

[13] S. Bastiaens, S. K. Goudos, W. Joseph, and D. Plets, "Metaheuristic optimization of LED locations for visible light positioning network planning," *IEEE Trans. Broadcast.*, vol. 67, no. 4, pp. 894–908, Dec. 2021.

[14] W. Gu, M. Aminikashani, P. Deng, and M. Kavehrad, "Impact of multipath reflections on the performance of indoor visible light positioning systems," *J. Lightw. Technol.*, vol. 34, no. 10, pp. 2578–2587, May 6, 2016.

[15] P. Du et al., "Experimental demonstration of 3D visible light positioning using received signal strength with low-complexity trilateration assisted by deep learning technique," *IEEE Access*, vol. 7, pp. 93986–93997, 2019.

[16] D. Shi et al., "Physics-based modeling of GaN MQW LED for visible light communication systems," *IEEE Trans. Electron Devices*, vol. 71, no. 1, pp. 337–342, Jan. 2024.

[17] H. Q. Tran and C. Ha, "Machine learning in indoor visible light positioning systems: A review," *Neurocomputing*, vol. 491, pp. 117–131, Jun. 2022.

[18] N. Knudde, W. Raes, J. De Bruycker, T. Dhaene, and N. Stevens, "Data-efficient Gaussian process regression for accurate visible light positioning," *IEEE Commun. Lett.*, vol. 24, no. 8, pp. 1705–1709, Aug. 2020.

[19] D. Plets et al., "Three-dimensional visible light positioning: An experimental assessment of the importance of the LED's locations," in *Proc. Int. Conf. Indoor Position. Indoor Navig. (IPIN)*, 2019, pp. 1–6.

[20] E. Aparicio-Esteve, W. Raes, N. Stevens, J. Ureña, and l. Hernández, "Experimental evaluation of a machine learning-based RSS localization method using Gaussian processes and a quadrant photodiode," *J. Lightw. Technol.*, vol. 40, no. 19, pp. 6388–6396, Oct. 1, 2022.

[21] R. Liu, Z. Liang, K. Yang, and W. Li, "Machine learning based visible light indoor positioning with single-LED and single rotatable photo detector," *IEEE Photon. J.*, vol. 14, no. 3, pp. 1–11, Jun. 2022.

[22] Y. Chen, W. Guan, J. Li, and H. Song, "Indoor real-time 3-D visible light positioning system using fingerprinting and extreme learning machine," *IEEE Access*, vol. 8, pp. 13875–13886, 2020.

[23] H. Q. Tran and C. Ha, "Fingerprint-based indoor positioning system using visible light communication—A novel method for multipath reflections," *Electronics*, vol. 8, no. 1, p. 63, 2019.

[24] T. H. Quang and C. Ha, "High precision weighted optimum K-nearest Neighbors algorithm for indoor visible light positioning applications," *IEEE Access*, vol. 8, pp. 114597–114607, 2020.

[25] Y.-C. Chuang, Z.-Q. Li, C.-W. Hsu, Y. Liu, and C.-W. Chow, "Visible light communication and positioning using positioning cells and machine learning algorithms," *Opt. Exp.*, vol. 27, no. 11, pp. 16377–16383, May 2019.

[26] A. M. Abdalmajeed, M. Mahmoud, A. E.-R. A. El-Fikky, H. A. Fayed, and M. H. Aly, "Improved indoor visible light positioning system using machine learning," *Opt. Quant. Electron.*, vol. 55, no. 3, p. 209, 2023.

[27] L. Polak, S. Rozum, M. Slanina, T. Bravenec, T. Fryza, and A. Pikrakis, "Received signal strength fingerprinting-based indoor location estimation employing machine learning," *Sensors*, vol. 21, no. 13, p. 4605, 2021. [Online]. Available: https://www.mdpi.com/1424-8220/21/13/4605

[28] Z. Zhang and C. Jung, "GBDT-MO: Gradient-boosted decision trees for multiple outputs," *IEEE Trans. Neural Netw. Learn. Syst.*, vol. 32, no. 7, pp. 3156–3167, Jul. 2021.

[29] L. Prokhorenkova, G. Gusev, A. Vorobev, A. V. Dorogush, and A. Gulin, "CatBoost: Unbiased boosting with categorical features," in *Proc. 32nd Int. Conf. Adv. Neural Inf. Process. Syst.*, vol. 31, 2018, pp. 6639–6649.

[30] T. Yang, Y.-F. Li, M. Mahdavi, R. Jin, and Z.-H. Zhou, "Nyström method vs random fourier features: A theoretical and empirical comparison," in *Proc. Adv. Neural Inf. Process. Syst.*, vol. 25, 2012, pp. 1–9.

[31] I. H. Sarker, "Machine learning: Algorithms, real-world applications and research directions," *SN Comput. Sci.*, vol. 2, no. 3, p. 160, 2021.

[32] G. Baudat and F. Anouar, "Kernel-based methods and function approximation," in *Proc. Int. Joint Conf. Neural Netw.*, 2001, pp. 1244–1249.

[33] C. Williams and M. Seeger, "Using the Nyström method to speed up kernel machines," in *Proc. Adv. Neural Inf. Process. Syst.*, vol. 13, 2000, pp. 1–7.

[34] V. Bellavista-Parent, J. Torres-Sospedra, and A. Pérez-Navarro, "Comprehensive analysis of applied machine learning in indoor positioning based on Wi-Fi: An extended systematic review," *Sensors*, vol. 22, no. 12, p. 4622, Jun. 2022. [Online]. Available: http://dx.doi.org/10.3390/s22124622

[35] M.-P. Hosseini, A. Hosseini, and K. Ahi, "A review on machine learning for EEG signal processing in bioengineering," *IEEE Rev. Biomed. Eng.*, vol. 14, pp. 204–218, 2021, doi: 10.1109/RBME.2020.2969915.

[36] H. Zhang, B. Hu, S. Xu, B. Chen, M. Li, and B. Jiang, "Feature fusion using stacked denoising auto-encoder and GBDT for Wi-Fi fingerprint-based indoor positioning," *IEEE Access*, vol. 8, pp. 114741–114751, 2020.

[37] I. D. Mienye and Y. Sun, "A survey of ensemble learning: Concepts, algorithms, applications, and prospects," *IEEE Access*, vol. 10, pp. 99129–99149, 2022.

[38] Y. Feng, L. Liu, and J. Shu, "A link quality prediction method for wireless sensor networks based on XGBoost," *IEEE Access, Pract. Innovat., Open Solut.*, vol. 7, pp. 155229–155241, 2019.

[39] D. Rani, N. S. Gill, P. Gulia, F. Arena, and G. Pau, "Design of an intrusion detection model for IoT-enabled smart home," *IEEE Access*, vol. 11, pp. 52509–52526, 2023.

[40] S. S. Prasad, R. C. Deo, N. Downs, D. Igoe, A. V. Parisi, and J. Soar, "Cloud affected solar UV prediction with three-phase wavelet hybrid convolutional long short-term memory network multi-step forecast system," *IEEE Access*, vol. 10, pp. 24704–24720, 2022.

[41] K. Yongcharoenchaiyasit, S. Arwatchananukul, P. Temdee, and R. Prasad, "Gradient boosting based model for elderly heart failure, aortic stenosis, and dementia classification," *IEEE Access*, vol. 11, pp. 48677–48696, 2023.

[42] D. Chanal, N. Y. Steiner, D. Chamagne, and M.-C. Pera, "Impact of standardization applied to the diagnosis of LT-PEMFC by fuzzy C-means clustering," in *Proc. IEEE Veh. Power Propuls. Conf. (VPPC)*, 2021, pp. 1–6.

[43] M. Despotovic, V. Nedic, D. Despotovic, and S. Cvetanovic, "Evaluation of empirical models for predicting monthly mean horizontal diffuse solar radiation," *Renew. Sustain. Energy Rev.*, vol. 56, pp. 246–260, Apr. 2016.

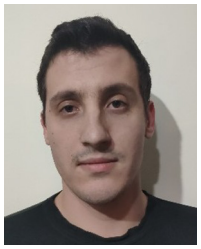

Vasileios P. Rekkas (Graduate Student Member, IEEE) received the B.Sc. degree in physics and the M.Sc. degree in electronic physics (radioelectrology) from the Aristotle University of Thessaloniki in 2017 and 2020, respectively, where he is currently pursuing the Ph.D. degree. His research interests lie in the areas of wireless communications, radio propagation, artificial intelligence techniques (machine learning, deep learning methods, and evolutionary algorithms), antenna design, and electromagnetics, while his Ph.D. research is funded by the Hellenic Foundation for Research and Innovation.

Sotirios P. Sotiroudis received the first B.Sc. degree in physics from the Aristotle University of Thessaloniki in 1999, the second B.Sc. degree in informatics from Hellenic Open University in 2011, and the M.Sc. degree in electronics and the Ph.D. degree in physics from the Aristotle University of Thessaloniki, in 2002 and 2018, respectively, where he worked with the Telecommunications Center from 2004 to 2010. He worked as a Teacher of physics and informatics with the Greek Ministry of Education from 2010 to 2022. He joined the Department of Physics, Aristotle University of Thessaloniki, in 2022. He has been involved in several research projects. His research interests include wireless communications, radio propagation, optimization algorithms, computer vision, and machine learning.

Lazaros Alexios Iliadis (Graduate Student Member, IEEE) received the B.Sc. degree in physics and the M.Sc. degree in electronic physics (radioelectrology) from the Aristotle University of Thessaloniki in 2017 and 2021, respectively, where he is currently pursuing the Ph.D. degree. His research interests include the development of the sixth generation communications systems (6G), antenna design and electromagnetics, artificial intelligence techniques (evolutionary algorithms, machine learning, and deep learning methods), and computer vision.

Sander Bastiaens received the M.Sc. and Ph.D. degrees in electrical engineering from Ghent University in 2017 and 2022, respectively, where his research focussed on centimetre-order indoor localisation with (unmodulated) visible light positioning and its industrial applications.

Wout Joseph (Senior Member, IEEE) was born in Ostend, Belgium, in October 1977. He received the M.Sc. degree in electrical engineering from Ghent University, Belgium, in July 2000, and the Ph.D. degree in March 2005. This work dealt with measuring and modeling of electromagnetic fields around base stations for mobile communications related to the health effects of the exposure to electromagnetic radiation. He was a Postdoctoral Fellow of the FWO-V Research Foundation, Flanders, from 2007 to 2012. Since October 2009, he has been a Professor in the domain of "Experimental Characterization of wireless communication systems." He is IMEC PI since 2017. His professional interests are electromagnetic field exposure assessment, propagation for wireless communication systems, antennas, and calibration. Furthermore, he specializes in wireless performance analysis and quality of experience.

David Plets (Member, IEEE) has been a member of the imec-WAVES Group, Department of Information Technology, Ghent University, since 2006, where he has also been a Professor since 2016. His current research interests include signal-strength and time-based localization techniques for various applications, the Internet-of-Things, and the characterization and optimization of wireless communication and broadcast networks, with a focus on coverage, exposure, and interference.

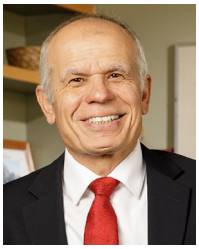

Christos G. Christodoulou (Life Fellow, IEEE) received the Ph.D. degree in electrical engineering from North Carolina State University in 1985.

He is currently with the Department of Electrical and Computer Engineering, University of New Mexico (UNM), where he serves as the Director of COSMIAC Research Center on Space Electronics. He is a member of Commission B of the U.S. National Committee for URSI, and a Distinguished Professor at UNM. He has published over 600 papers in journals and conferences, written 19 book chapters, co-authored nine books, and has several patents. Over his academic career he has served as the major advisor for over 40 Ph.D. and 75 M.S. students.

Dr. Christodoulou is the recipient of the 2010 IEEE John Krauss Antenna Award for his work on reconfigurable fractal antennas using MEMS switches and has been inducted in the Alumni Hall of Fame for the Electrical and Computer Engineering Department, at North Carolina State University, in 2016. He was appointed as an IEEE AP-S Distinguished Lecturer from 2007 to 2010 and served as an Associate Editor for the IEEE TRANSACTIONS ON ANTENNAS AND PROPAGATION for six years. He served as a Co-Editor for a special issue on "Reconfigurable Systems" in the IEEE Proceedings, March 2015, a Co-Editor of the IEEE Antennas and Propagation Special issue on "Synthesis and Optimization Techniques in Electromagnetics and Antenna System Design" March 2007, and for the Special issue on "Antenna Systems and Propagation for Cognitive Radio" in 2014. Since 2013, he has been serving as the Series Editor for Artech House Publishing company for the areas of Antennas, Propagation, and Electromagnetics.

George K. Karagiannidis (Fellow, IEEE) is currently a Professor with the Electrical and Computer Engineering Department, Aristotle University of Thessaloniki, Greece, and the Head of Wireless Communications and Information Processing Group. He is also a Faculty Fellow with the Artificial Intelligence and Cyber Systems Research Center, Lebanese American University. His research interests are in the areas of wireless communications systems and networks, signal processing, optical wireless communications, wireless power transfer and applications and communications, and signal processing for biomedical engineering. Recently, he received three prestigious awards: The 2021 IEEE ComSoc RCC Technical Recognition Award, the 2018 IEEE ComSoc SPCE Technical Recognition Award, and the 2022 Humboldt Research Award from Alexander von Humboldt Foundation. He is one of the highly-cited authors across all areas of Electrical Engineering, recognized from Clarivate Analytics as Web-of-Science Highly-Cited Researcher from 2015 to 2023. He is an Editor-in Chief of the IEEE TRANSACTIONS ON COMMUNICATIONS and in the past was an Editor-in Chief of IEEE COMMUNICATIONS LETTERS.

Sotirios K. Goudos (Senior Member, IEEE) received the B.Sc. degree in physics and the first M.Sc. degree in electronics from the Aristotle University of Thessaloniki, Thessaloniki, Greece, in 1991 and 1994, respectively, the second M.Sc. degree in information systems from the University of Macedonia, Greece, in 2005, and the Ph.D. degree in physics and the Diploma degree in electrical and computer engineering from the Aristotle University of Thessaloniki in 2001 and 2011, respectively.

He is a Professor with the Department of Physics of Aristotle University of Thessaloniki. He is the Director of the ELEDIA@AUTH Lab and the member of the ELEDIA Research Center Network. He is the Founding Editor-in-Chief of *Telecom Open-Access Journal* (MDPI Publishing). He is currently serving as an Associate Editor for *IEEE Transactions on Antennas and Propagation*, IEEE ACCESS, and *IEEE open journal of the communication society*. He is the author of the book *Emerging Evolutionary Algorithms for Antennas and Wireless Communications* and Institution of Engineering & Technology in 2021.